DOI: 10.1007/s11099-016-0663-2 PHOTOSYNTHETICA 55 (3): 434-442, 2017

Morphological recognition with the addition of multi-band fluorescence excitation of chlorophylls of phytoplankton

M. LAUFFER[*,**], F. GENTY[*,**], S. MARGUERON[**,*], and J.L. COLLETTE[***]

LMOPS, EA n°4423, Centrale Supélec, 2 rue Edouard Belin, Metz, 57070, France[*]
LMOPS, EA n°4423, Université de Lorraine, 2 rue Edouard Belin, Metz, 57070, France[**]
IMS group, Centrale Supélec, UMI n°2958 Georgia Tech/CNRS, 2 rue Edouard Belin, Metz, 57070, France[***]

Abstract

The recognition of aquatic organisms plays a crucial role in the monitoring of the pollution and for the adoption of rapid preventive actions. A compact microscopic optical imaging system is proposed in order to acquire and treat the multi-bands fluorescence of several pigments in phytoplankton organisms. Two algorithms for automatic recognition of phytoplankton were proposed with a minimum number of calibration parameters. The first algorithm provides a morphological recognition based on "watershed" segmentation and Fourier descriptors, while the second one builds fluorescence pigment images by "k-means" partition of intensity ratios. The operation of these algorithms was illustrated by the study of two different organisms: a cyanobacteria (*Dolichospermum* sp.) and an alga (*Cladophora* sp.). The family and the genus of these organisms were then classified into a database which is independent of the size, the orientation and the position of the specimens in the images.

Additional key words: aquatic organism; fluorescence imaging; morphological extraction; pigment.

Introduction

Phytoplankton plays a fundamental role in the living world. It is a dioxygen generator and the most important carbon dioxide fixer on the Earth. However, in the case of the blooming of algae, their development may become so excessive that it can be harmful to other aquatic plants and animals. This phenomenon, called hyper-eutrophication (Codd *et al*. 2005, Hudnell 2008), reduces photosynthesis and gas exchange and can cause the death of the whole aquatic ecosystem (Vasconcelos 1999, Falconer and Humpage 2005). Moreover, many of the invasive species can also present a risk for human health (Batoréu *et al* 2005, Metcalf *et al*. 2012). Especially, some cyanobacteria are toxic due to their ability to produce dermatotoxins, hepatotoxins or neurotoxins. The death of fishes but also the poisoning of cattle and humans have been reported (Quiblier *et al*. 2013). It appears therefore essential to strengthen the vigilance on the control of the proliferation of phytoplankton and toxins with the necessity to evaluate the risk of invading species. The recognition and the identification of aquatic organisms, necessary for such a control, are often performed by algologist – specialists by means of sampling and visual microscopic observations. The number of analyses is limited and depends on the limited number of specialists. Nevertheless, under certain circumstances, it may be useful to develop an *in situ* monitoring system which would provide an autonomous and automatic recognition algorithm to improve the monitoring of risky water ponds and optimize human intervention of specialists. The development of such an automatic system of recognition of aquatic algae and cyanobacteria by irradiance reflectance (Gons *et al*. 2005), by fluorescence measurement (Poryvkina *et al*. 2000), or again by image recognition (Tang *et al*. 1998), is more and more considered.

However, only few studies have been reported on the fluorescence imaging methods and the data treatments. Imaging methods based on chlorophyll (Chl) *a* fluorescence have been evaluated for the understanding of photosynthesis mechanism (Bro *et al*. 1996, Lichtenthaler *et al*. 2005, Lichtenthaler *et al*. 2007, Guidi and Degl'Innocenti 2011, van Wittenberghe *et al*. 2013), to detect the stress in plants (Zarco-Tejada *et al*. 2009) or to describe the dynamical and spatial behavior in plants (Chaerle *et al*. 2007). From the sensor's point of view, most of the

Received 31 March 2016, *accepted* 15 July 2016, *published as online-first* 5 October 2016.
+Corresponding author; e-mail: mathieu.lauffer@centralesupelec.fr
Abbreviations: CCD – charge coupled device; Chl – chlorophyll.
Acknowledgements: This work was supported by Europe (FEDER), Lorraine region and the project "BioCapTech". The authors wish to thank emeritus Pr. Jean-Claude Pihan and Dr Cécile Dupouy (IRD, Nouméa) for their advices during the course of this study.

fluorescence studies are based on macroscopic and averaging spectral studies using spectrofluorimetry (Yentsch and Phinney 1985, See *et al*. 2005, Richardson *et al*. 2010, Ziegmann *et al*. 2010). These methods are usually very efficient to estimate the concentration of Chl *a* in an aquatic environment (Seppälä *et al*. 2000, Seppälä *et al*. 2007) but remain not selective enough to distinguish algae or cyanobacteria species. Only recognition at the family level is possible.

In this study, we presented a multi-band fluorescence imaging system in order to study two different aquatic organisms as examples: a Chlorophycea (*Cladophora* sp.) and a Cyanobacteria (*Dolichospermum* sp.). The first step is to take fluorescence images of different pigments of this phytoplankton (Chl *a*, Chl *b*, and the combination of both). By selecting the proper absorption and a fluorescence wavelength in the range of study, the system enables to perform images for each pigment with a high selectivity. The image processing algorithms are then applied on the fluorescence images but also on classical microscopy (white light illumination) images to provide the morphologic characteristics and the intensities of the pigments of both the organisms. Finally, the treatment of the different phytoplankton images is used to develop a database of algae and cyanobacteria. This database has been extended to contain 27 species but only two species were presented in our fluorescence analysis.

Materials and methods

Sample preparations: Cyanobacteria (*Dolichospermum* sp.) grown in nutrient rich solution for one month have been provided by *F. P. Environnement* (Merten, France). ALATOX (chlorophyll measurement by fluorescence) measurements showed a concentration of 89.68 µg(Chl) L^{-1}, *i.e*., 2.813,700 cells mL^{-1}. Concerning the second aquatic organism, the Chlorophycea (*Cladophora* sp.), the studied specimens was collected during the spring 2014 in the Seille, a tributary river of the Moselle, in Metz, Lorraine, France. The measurements were done on the fresh specimen of *Cladophora* sp. In order to preserve the properties of the living specimen, all samples were stored in the shade at 6°C and analyzed alive.

Fluorescence imaging system: The fluorescence imaging system was a home-made setup operating in transmission (Fig. 1). A metallographic microscope was illuminated by the top with a Kohler's illumination mounting. The excitation was provided by an ultraviolet lamp (*OmniCure S1000*, 100 W, 250–500 nm, *Lumen Dynamics,* Canada). In order to select the fluorescence excitation we used band pass filters at 400 ± 10 nm (absorption of Chl *a*) (Chen and Blankenship 2011), at 440 ± 10 nm (absorption of Chl *a* and Chl *b*) (Rabinowitch and Govindjee 2013) and at 475 ± 10 nm (absorption of Chl *b*) (Shedbalkar and Rebeiz 1992). The excitation power densities was of about 50 mW cm^{-2}.

The data acquisitions were performed with microscope objectives plan (*Optika*, Italia) × 20 (NA = 0.40), × 60 (NA = 0.85), and × 100 (NA = 1.25). Fluorescence emission was selected by a red broadband filters (650–700 nm). This setup enabled us to detect the Chl *a* which emits at a maximum of 673 nm when diluted in organic solvent (Wörmke *et al*. 2007, Falco *et al*. 2011) and in the 680–685 nm when it is present in alive cells (Govindjee and Shevela 2011). Also the Chl *b* emits at a maximum of 651 nm (Trytek *et al*. 2011). For the detection, we used a 8-bit monochromatic camera with 2,048 × 1,536 pixel CCD sensor (*PixeLINK,* Canada). Because of the turbidity and the cells concentration, the solution was dropped on a transparent sapphire cover prior to the measurements. The focus of the microscope was done manually on the chloroplast of the living cells and several images were acquired at different wavelengths by turning the wheel filters.

Data treatments: All the data processing presented here was done on *Matlab*® using an image processing library. The different operations performed in the result section were defined as following.

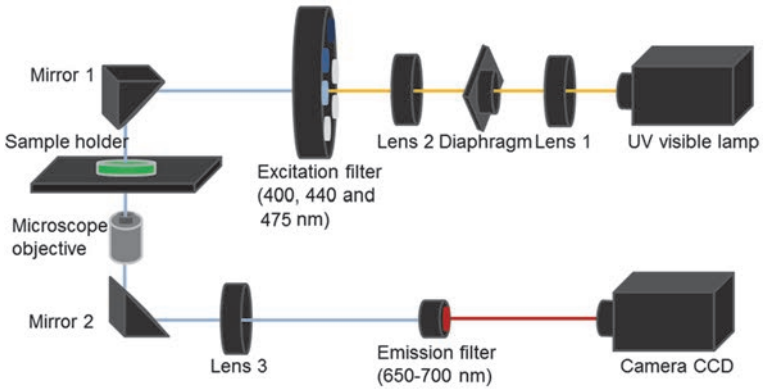

Fig. 1. Optical set-up for fluorescence imaging.

Image segmentation: Each image was a grayscale image I(x,y) coded on 8 bits (intensity range). The data treatment was later applied on the derivative of the image to subtract the continuous component and identify the frontiers of the cells (Chen 2007, Wang *et al*. 2010, 2011). Moreover, the gradient of the images $I_d(x,y)$ was computed by taking into account the convolution by a 2D Gaussian filter to minimize the noise. To optimize the speed of the algorithm, the gradient of the image was calculated by considering the derivative on the 2D spatial components, x (respectively y component), and smoothed by the convolution of a Gaussian band pass filter along y (resp. x) and the derivative of the Gaussian filter along x (resp. y). We applied the Gaussian filter on the first neighbor with a standard deviation σ = 1.3 (in pixel unit) and a dimension of the numeric filter of GN = 4. This reduced the noise in the image and highlighted the boundaries in the image.

Watershed: The segmentation of images I_d was obtained with the "watershed" function which can suppress all the minima whose depth are less than the parameter h, using the "imhmin" function. The parameter h must be defined previously by the user. In our simulations, h = 0.004 gave good segmentation on all specimens. This segmentation process was used for the morphological recognition of algae and for fluorescence images analysis as described further.

Erosion: For the morphological recognition, the "watershed" segmentation was applied on the previous gradient of the image. The boundaries of the greatest object can then be obtained using the "bw boundaries" function and enable the definition of the external contour of this object.

Fourier descriptor: The closed contour of the object defined a list of N coordinates (x_n,y_n) that can be represented by a series of complex numbers:

$$z_n = x_n + iy_n \quad (1)$$

The contour can be represented by a periodic function of period N. Then the contour can be approximated by:

$$\hat{z}_m = \bar{z} + \sum_{-kmax}^{kmax} a_k \exp\left(\frac{2\pi jkm}{N}\right) \quad (2)$$

with $\bar{z}$ the average signal, and a_k the Fourier coefficients. We computed the function using Fast Fourier Transform function and defining k_{max} = 10. The coefficients were permuted in such a way as to be independent of the position, orientation and normalized in order to be independent of the scaling factor (Hall 1979). The Fourier descriptors defined also one contour for one sample with many coefficients.

k-means: In order to analyze the different intensities of the fluorescence images, the image was treated by k-means function to make a partition of k = 10 clusters of intensities (Yao *et al*. 2013).

Results

The microscopic acquisition of the images on Cyanobacteria (*Dolichospermum* sp.) and Chlorophycea (*Cladophora* sp.) were done consecutively on the same specimens. Two automatic recognition procedures were then applied. We named furher the images collected with the full illumination of the lamp and no emission filter as "white-light images". The images taken with the selected emission filters with the excitation (400/440/475 nm) (Shedbalkar and Rebeiz 1992, Chen and Blankenship 2011, Rabinowitch and Govindjee 2013) and the emission filters at 650–700 nm (Wörmke *et al*. 2007, Falco *et al*. 2011, Govindjee and Shevela 2011, Trytek *et al*. 2011) were called further "fluorescence images". Due to the mobility of the living organisms and the relatively long manual procedure, some of the fluorescence images may have been reoriented or translated to fit the "white-light image". Also, in order to optimize the rate of the algorithm, we defined cluster areas on the "white-light images" to be applied as a pencil on the different "fluorescence images". The two procedures of automatic treatments were presented further.

Automatic recognition of morphological parameters: The automatic recognition process enabled to extract several morphological characteristics of the organisms that can be collected into a database. First, the procedure was applied on "white-light images" of Chlorophycea (*Cladophora* sp., Fig. 2*A*) and Cyanobacteria *(Dolicho-spermum* sp*.,* Fig. 2*C)*. The "watershed" segmentation on the image derivative are presented in Fig 2*B* and *D*, respectively. As several other impurities and pollution may corrupt the sample, the aquatic organism was supposed to be the largest region of the segmented image. Conse-quently, all the other regions were later removed by erosion algorithm. The analysis of *Cladophora* sp. (Fig. 2*B*) showed that the algae overfilled the edges of the CCD image. Moreover, one could note that minor impurities link the two specimens together, which generates an unrealistic specimen. As a consequence, this kind of images did not present an interest for morphological analysis and was only analyzed by fluorescence imaging. Concerning *Dolichospermum* sp. (Fig. 2*D*), the whole profile of the cyanobacteria could be

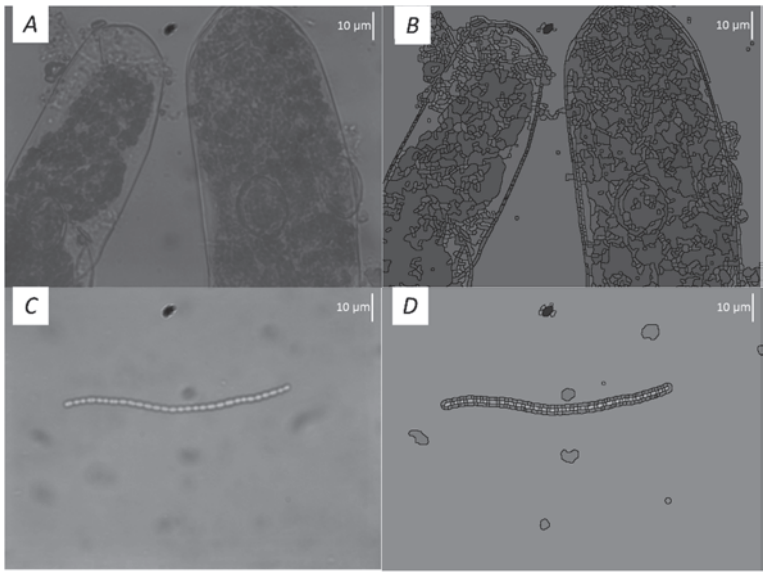

Fig. 2. On the left, "white light" and unfiltered microscopic image with × 20 and × 60 magnification objective respectively for *Cladophora* sp. (*A*) and *Dolichospermum* sp. (*C*), and on the right, same image after derivation. Gaussian filter and segmentation by watershed function with h = 0.004 (*B*,*D*).

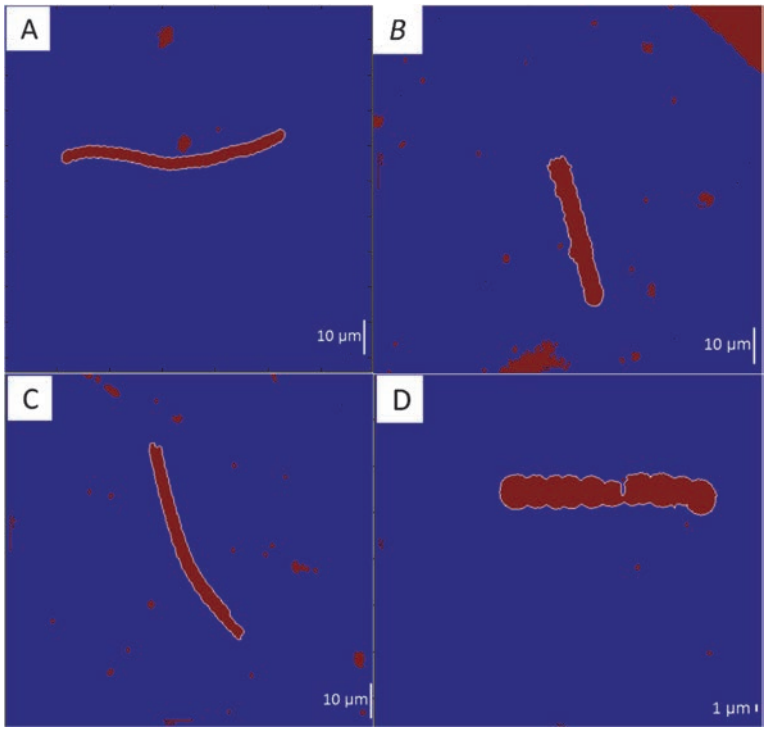

Fig. 3. Extracted images of the largest regions of the merged watershed segmentation of *Dolichospermum* sp. Cyanobacteriae. Images *A*, *B*, and *C* are acquired with × 60 magnification and *D* is acquired with × 100 magnification objective.

observed on the images with minor impurities and it was therefore a correct image for the outline algorithm. This later specimen was then used in the following steps.

To illustrate the Fourier descriptor method, four different images of *Dolichospermum* sp. were presented with × 60 magnification (Fig. 3*A*–*C*) and with × 100 magnification (Fig. 3*D*). The cyanobacteria were classified using the Fourier coefficients (Fig. 4*B*,*C*), respectively, with the real part and the imaginary part of normalized coefficients. The imaginary part appeared not to be very significant in this case because it described mainly defects on the edge and heterogeneities. On the contrary, the real part defined from 20 coefficients was very significant for this cyanobacterium. The highest intensities were obtained for the coefficients 1 and −1. Based on this process, we determined the shape of the organisms (Fig. 4*A*). The rotation of π for each shape was also considered in order to improve the database. As a consequence, eight Fourier descriptors were extracted (Fig. 4*A*). Owing to the Fourier descriptor method, several characteristic morphological parameters, such as length, width, perimeter, and surface could be extracted. In addition, the ratios between these different parameters were also valuable characteristic parameters of algae for the database.

Therefore, the shapes of *Dolichospermum* sp. extracted as described previously, could be used to distinguish other

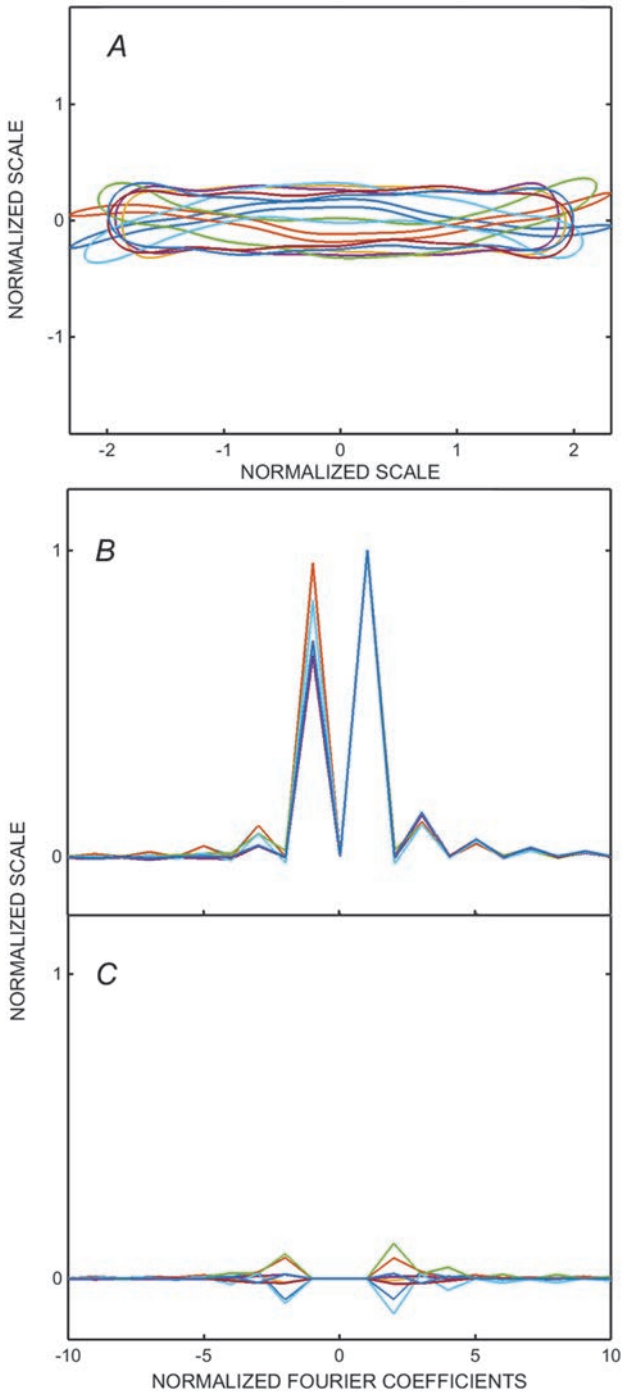

Fig. 4. Top of figure, normalized shapes of the four specimens of *Dolichospermum* sp. (*A*) with the replicate of each by n rotation, and, at the bottom, amplitudes *vs*. frequencies of the Fourier coefficients of the four outlines on the real part (*B*), and on the imaginary part (*C*).

Discussion

The imaging system and algorithms described in the present paper were developed to improve the recognition of aquatic organisms. The segmentation based on morphological characteristics is close to the visual recognition by the algologists and enables to extract size and shape of algae and cyanobacteria (van den Hoek 1963, Komárek aquatic organisms which are not filamentous as unicellular organisms or colonial organisms. In particular, the width appeared to be a specific parameter for a *Dolichospermum* sp. recognition but the length of the filament could vary depending on the cyanobacteria specimen observed. One can also notice that the use of the higher magnification objective enabled to obtain with more details of the shape of the spherical cells which compose the filaments (Fig. 3*D*). Such a procedure was applied at × 100 magnification (Fig. 3*D*) and × 60 magnification (Fig. 3*A*–*C*). With the × 100 magnification, it was possible to determine very few segmented regions which could limit the recognition error but such a procedure remained technically more difficult for an operator or an automatic focusing.

Automatic recognition by multi-bands fluorescence excitation: It was clearly visible that the regions, which exhibited high fluorescence intensities, were localized in the chloroplasts (Fig. 5). In this case, the fluorescence emission brought information about the composition of the alga but also about the shape of the chloroplasts. These new parameters were characteristic of the alga and gave additional accuracy in the framework of a morphological recognition. One can also notice that the impurities in between the cells did not emit any fluorescence. It is known that the Chlorophyceae contains a majority of Chl *a* and Chl *b* (Fig. 5). However, the absolute intensity was difficult to use for a sensor since the excitation and emission wavelengths are very close to each other for the different Chl pigments (and the pass-band filters was not narrow enough) which could induce errors from parasitic or scattering light (Fig. 5*C*). As a consequence and in order to avoid such errors, the fluorescence ratios of the pigments on each segment area were used. These ratios appeared to be specific to a given alga (*Cladophora* sp. in this case) and were an operational parameter for automatic recognition (Fig. 7*A*).

A similar treatment was also applied on *Dolichospermum* sp. The fluorescence imaging of the three pigments (Chl *a*, Chl *b* and the combination of two) are presented in Fig. 6. In this case, the cyanobacteria contained Chl *a* and Chl *a* + *b* but no fluorescence of Chl *b* which was well represented by the fluorescence imaging. As already pointed out in the case of Chlorophycea, the shape of the chloroplasts in Fig. 6*A* was well delimited by the fluorescence of Chl *a*. Then, the spherical shape of these chloroplasts can be observed which was a characteristic of *Dolichospermum* sp.

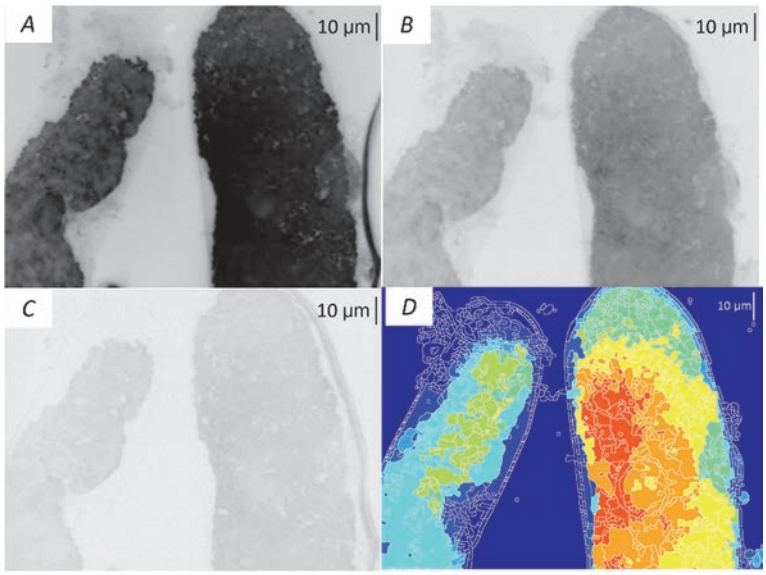

Fig. 5. Fluorescence images of *Cladophora* sp. with an excitation at 440 nm for chlorophyll *a* + *b* (*A*), at 475 nm for chlorophyll *b* (*B*), at 400 nm for chlorophyll *a* independently (*C*) and image of segmentation by "k-means" of the fluorescence images of the three bands [chlorophyll (*a*+*b*), chlorophyll *b*, and chlorophyll *a*] (*D*).

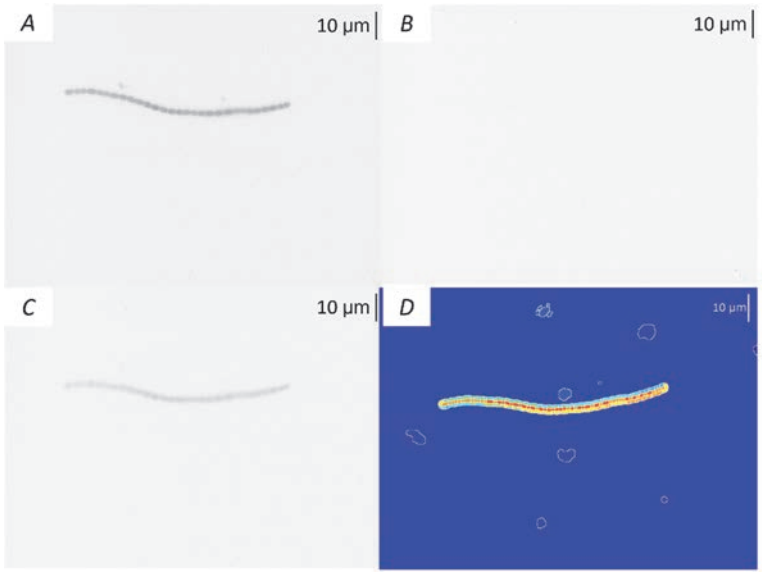

Fig. 6. Fluorescence images of *Dolichospermum* sp. with an excitation at 440 nm for chlorophyll *a* + *b* (*A*), at 475 nm for chlorophyll *b* (*B*), at 400 nm for chlorophyll *a* independently (*C*) and image of segmentation by "k-means" of the fluorescence images of the three bands [chlorophyll (*a*+*b*), chlorophyll *b*, and chlorophyll *a*] (*D*).

and Anagnostidis 2000, Wacklin 2009). The different morphological parameters extracted from the segmentation of the images have been used to create a database usable for automatic recognition of aquatic organisms (27 species). As demonstrated previously, the use of this database should enable the simple automatic recognition of phytoplankton and cyanobacteria by a non-specialist.

Moreover, the multispectral imaging provided additional information. For *Cladophora* sp., the fluorescence showed the predominant presence of Chl *a* and the secondary presence of Chl *b*. These observations confirmed the classical composition of pigments in Chlorophyceae (Wilhelm and Lenarz-Weiler 1987). Together with the intensity and emission wavelength, the fluorescence imaging enabled to extract the shape of chloroplast which can be different from the shape of the filament or the cells. Such additional morphological information can then be extracted to extend the database.

In the second experiment, the presence of Chl *a* and the absence of Chl *b* confirmed the classical composition of pigments in cyanobacteria (Kühl 2005). Chl *b* is not referred as a pigment in cyanobacteria and no intensity of fluorescence was detected. In the same way, the segmentation of fluorescence intensities revealed that the majority of pigments was Chl *a* and the inner cell showed well-defined shape of chloroplasts from where the fluorescence emission originated. Therefore, morphological characteristics can also be extracted from the segmentation and processing of the fluorescence intensity images.

The fluorescence intensities ratio plotted in three dimensions along the three bands of Chl *a*, *b* and combination of two was shown in Fig. 7. Such a spectral signature is unique for each organism and can be used for algae recognition. Moreover, the use of this parameter limited the errors of interpretation eventually originating from absolute intensity study as in the case of

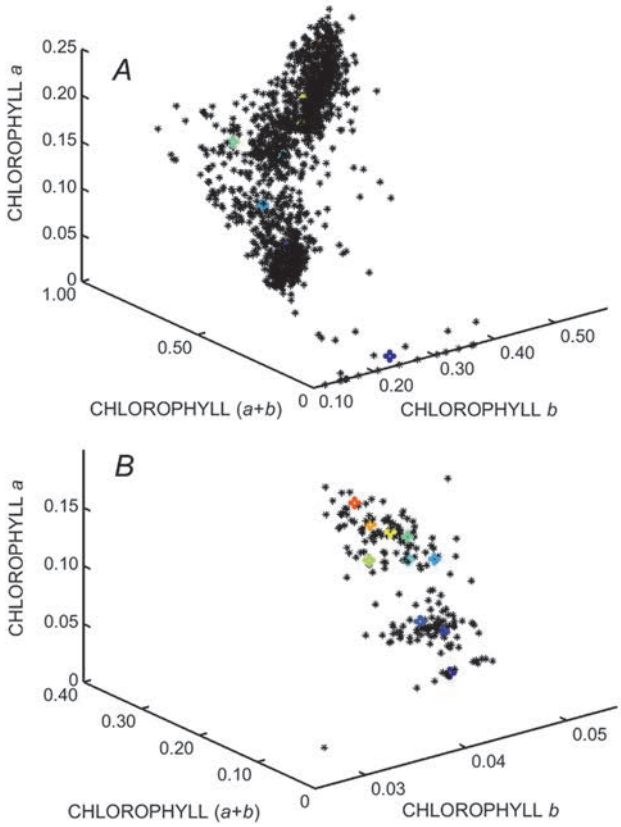

Fig. 7. Fluorescence intensity ratios in 3D normalize between 0 and 1, and obtained from k-mean areas of the image and corresponding to the three emission bands [chlorophyll *a*, chlorophyll (*a*+*b*), and chlorophyll *b*] observed in *Cladophora* sp. above (*A*) and *Dolichospermum* sp. below (*B*).

Dolichospermum sp. That way, in the case of *Cladophora* sp., the ratio between Chl *b* and Chl *a* was specific. Despite a weak quantity of emission in *Dolichospermum* sp., the typical intensity profile deduced from the three bands map led to the establishment of characteristic data for these cyanobacteria.

From a practical point of view, the main difficulty for such an automatic recognition in natural environment is linked to the turbidity of water and the presence of impurities in the aquatic environment (Kutser 2006). To overcome this problem, morphological treatments are based on selected regions which must correspond to the target species only. The selection of the largest region after segmentation treatment by watershed and eventually an increase of the magnification generally avoided the problem linked to impurities. Concerning the problem of turbidity, it can be resolved with a wide dilution of the swab. An increase of the magnification could also limit this problem but the acquisition becomes more and more difficult due to the optical focalization.

As described previously, the narrowness of absorption and emission bands of Chl pigments (Shedbalkar and Rebeiz 1992, Wörmke *et al*. 2007, Chen and Blankenship 2011, Falco *et al*. 2011, Govindjee and Shevela 2011, Trytek *et al* 2011, Rabinowitch and Govindjee 2013) enabled to perform a multi-band imaging observation. Inthe same way, this recognition model based on Chls, can be extended to other molecules, such as carotenoids or phycobilins (French and Young 1952, McConnell *et al*. 2002, Stamatakis *et al*. 2014).

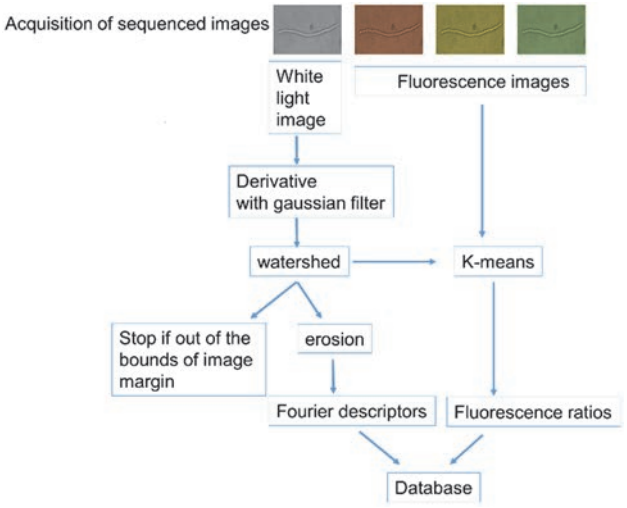

Fig. 8. Algorithm for automatic recognition of phytoplankton, described by morphological processing and ratio of fluorescence intensities.

Conclusion: The microscopic 'white-light images' and 'fluorescence images' of phytoplankton exhibited morphological and fluorescence characteristics of phytoplankton that enabled to identify the families and the genus of each specimen. The core method was to process the images using two automatic recognition algorithms. The morphological treatments were independent of the size and orientation of the specimens during acquisition and required only one parameter for segmentation. The outlines of the organisms were analyzed with Fourier descriptors. The analysis of fluorescence images provided the ratios of pigments in the cell and the chloroplasts. The morphological parameters, the Fourier descriptors and the information on pigment ratios were implemented to provide a database of aquatic organisms.

Two different solutions containing different organisms were tested with this automatic recognition system (Fig. 8). By means of this process, *Dolichospermum* sp. and *Cladophora* sp. were successfully recognized from a morphological point of view thanks to the optical microscopy analysis of their shape and from a fluorescence emission point of view by the determination of their chlorophyll compositions related to the shapes of their chloroplasts.

References

Batoréu M.C.C., Dias E., Pereira P. *et al.*: Risk of human exposure to paralytic toxins of algal origin. – Environ. Toxicol. Phar. **19**: 401-406, 2005.

Bro E., Meyer S., Genty B.: Heterogeneity of leaf CO_2 assimilation during photosynthetic induction. – Plant Cell Environ. **19**: 1349-1358, 1996.

Chaerle L., Leinonen I., Jones H.G. *et al.*: Monitoring and screening plant populations with combined thermal and chlorophyll fluorescence imaging. – J. Exp. Bot. **58**: 773-784, 2007.

Chen M., Blankenship R.E.: Expanding the solar spectrum used by photosynthesis. – Trend. Plant Sci. **16**: 427-431, 2011.

Chen X.: Skin lesion segmentation by an adaptive watershed flooding approach. – PhD Dissertation, Univ. Missouri-Rolla, 2007.

Codd G.A., Lindsay J., Young J.M. *et al.*: Harmful Cyanobacteria. – In: Huisman J., Matthijs H.C.P., Visser P.M. (ed.): Harmful Cyanobacteria. Pp. 1-23. Springer, Dordrecht 2005.

Falco W.F., Botero E.R., Falcão E.A. *et al.*: *In vivo* observation of chlorophyll fluorescence quenching induced by gold nanoparticles. – J. Photoch. Photobio. A **225**: 65-71, 2011.

Falconer I. R., Humpage A. R.: Health risk assessment of Cyanobacterial (blue-green algal) toxins in drinking water. – Ini. J. Env. Res. Pub. He. **2**: 43-50, 2005.

French C.S., Young V.K.: The fluorescence spectra of red algae and the transfer of energy from phycoerythrin to phycocyanin and chlorophyll. – J. Gen. Physiol. **35**: 873-890, 1952.

Gons H. J., Hakvoort H., Peters S. W. M. *et al.*: Optical detection of Cyanobacterial blooms. – In: Huisman J., Matthijs H.C.P., Visser P.M. (ed.): Harmful Cyanobacteria. Pp. 177-200. Springer, Dordrecht 2005.

Govindjee, Shevela D.: Adventures with Cyanobacteria: a personal perspective. – Front. Plant Sci. **2:** 1-17, 2011.

Guidi L., Degl'Innocenti E.: Imaging of chl *a* fluorescence: a tool to study abiotic stress in plants. – In: Shanker A., Venkateswarlu B. (ed.): Abiotic Stress in Plants – Mechanisms and Adaptations. Pp. 3-20. In Tech, 2011.

Hall E. L.: Computer Image Processing and Recognition. Pp. 585. Academic Press, New York 1979.

Hudnell H. K.: Cyanobacterial Harmful Algal Blooms: State of the Science and Research Needs: State of the Science and Research Needs. Pp. 2-15. Springer Sci. Business Media, New York 2008.

Komárek J., Anagnostidis K.: [Freshwater Flora of Central Europe: Chroococcales.] Pp. 548. Gustav Fischer Verlag, Stuttgart 2000. [In German]

Kühl M., Chen M., Ralph P.J. *et al.*: Ecology: a niche for Cyanobacteria containing chlorophyll *d*. – Nature **433:** 820-820, 2005.

Kutser T., Vahtmäe E., Martin G.: Assessing suitability of multispectral satellites for mapping benthic macroalgal cover in turbid coastal waters by means of model simulations. – Estuar. Coast. Shelf S. **67**: 521-529, 2006.

Lichtenthaler H.K., Langsdorf G., Lenk S. *et al.*: Chlorophyll fluorescence imaging of photosynthetic activity with the flash-lamp fluorescence imaging system. – Photosynthetica **43**: 355-369, 2005.

Lichtenthaler H.K., Babani F., Langsdorf G.: Chlorophyll fluorescence imaging of photosynthetic activity in sun and shade leaves of trees. – Photosynth. Res. **93**: 235-244, 2007.

McConnell M.D., Koop R., Vasil'ev S. *et al.*: Regulation of the distribution of chlorophyll and phycobilin-absorbed excitation energy in Cyanobacteria. – A structure-based model for the light state transition. – Plant Physiol. **130**: 1201-1212, 2002.

Metcalf J.S., Richer R., Cox P.A. *et al.*: Cyanotoxins in desert environments may present a risk to human health. – Sci. Total Environ. **421**: 118-123, 2012.

Poryvkina L., Babichenko S., Leeben A.: Analysis of phytoplankton pigments by excitation spectra of fluorescence. – EARSeL eProceedings **1**: 224-232 2000.

Quiblier C., Wood S., Echenique-Subiabre I. *et al.*: A review of current knowledge on toxic benthic freshwater Cyanobacteria – Ecology, toxin production and risk management. – Water Res. **47**: 5464-5479, 2013.

Rabinowitch E., Govindjee U.: Photosynthesis. Pp. 102-123. John Wiley & Sons, New York 2013.

Richardson T.L., Lawrenz E., Pinckney J.L. *et al.*: Spectral fluorometric characterization of phytoplankton community composition using the Algae Online Analyser®. – Water Res. **44**: 2461-2472, 2010.

See J.H., Campbell L., Richardson T.L. *et al.*: Combining new technologies for determination of phytoplankton community structure in the Northern Gulf of Mexico. – J. Phycol. **41**: 305-310, 2005.

Seppälä J., Ylöstalo P., Kaitala S. *et al.*: Ship-of-opportunity based phycocyanin fluorescence monitoring of the filamentous Cyanobacteria bloom dynamics in the Baltic Sea. – Estuar. Coast. Shelf S. **73**: 489-500, 2007.

Seppälä J., Babichenko S., Leeben A. *et al.*: Fluorescence diagnostics of phytoplankton bloom in Baltic, Institute of Ecology, Tallinn Estonia. – In: Proceedings of the Six International Conference on Remote Sensing for Marine and Coastal Environments. Pp. 377-383. Environmental Research Institute of Michigan, Ann Arbor 2000.

Shedbalkar V.P., Rebeiz C.A.: Chloroplast biogenesis: Determination of the molar extinction coefficients of divinyl chl *a* and *b* and their pheophytins. – Anal. Biochem. **207**: 261-266, 1992.

Stamatakis K., Tsimilli-Michael M., Papageorgiou G.C.: On the question of the light-harvesting role of β-carotene in photosystem II and photosystem I core complexes. – Plant Physiol. Bioch. **81**: 121-127, 2014.

Tang X., Stewart W. K., Vincent L. *et al.*: Automatic plankton image recognition. – In: Panigrahi S., Ting K.C. (ed.): Artificial Intelligence for Biology and Agriculture. Pp. 177-199. Springer, Dordrecht 1998.

Trytek M., Janik E., Maksymiec W. *et al.*: The spectral and catalytic studies of chlorophylls and pheophytins in mimetic biotransformation of α-pinene. – J. Photoch. Photobio. A **223:** 14-24, 2011.

van den Hoek C.: Revision of the European Species of Cladophora. Pp. 363. Brill Acad. Publ., Leiden 1963.

van Wittenberghe S., Alonso L., Verrelst J. *et al.*: Upward and downward solar-induced chlorophyll fluorescence yield indices of four tree species as indicators of traffic pollution in Valencia. – Environ. Pollut. **173**: 29-37, 2013.

Vasconcelos V.M.: Cyanobacterial toxins in Portugal: effects on aquatic animals and risk for human health. – Braz. J. Med. Biol. Res. **32**: 249-254, 1999.

Wacklin P., Hoffmann L., Komárek J.: Nomenclatural validation of the genetically revised Cyanobacterial genus *Dolichospermum* (Ralfs ex Bornet et Flahault) comb. – Fottea **9**: 59-64, 2009.

Wang H., Moss R.H., Chen X. *et al*.: Watershed segmentation of dermoscopy images using a watershed technique. – Skin Res. Technol. **16**: 378-384, 2010.

Wang H., Moss R.H., Chen X. *et al*.: Modified watershed technique and post-processing for segmentation of skin lesions in dermoscopy images. – Comput. Med. Imag. Grap. **35**: 116-120, 2011.

Wilhelm C., Lenarz-Weiler I.: Energy transfer and pigment composition in three Chl *b*-containing light-harvesting complexes isolated from *Mantoniella squamata* (Prasinophyceae), *Chlorella fusca* (Chlorophyceae) and *Sinapis alba*. – Photosynth. Res. **13**: 101-111, 1987.

Wörmke S., Mackowski S., Brotosudarmo T. H. *et al*.: Monitoring fluorescence of individual chromophores in peridinin–chlorophyll–protein complex using single molecule spectroscopy. – BBA-Bioenergetics **1767**: 956-964, 2007.

Yao H., Duan Q., Li D. *et al*.: An improved K-means clustering algorithm for fish image segmentation. – Math. Comput. Model. **58**: 790-798, 2013.

Yentsch C.S., Phinney D.A.: Spectral fluorescence: an ataxonomic tool for studying the structure of phytoplankton populations. – J. Plankton Res. **7**: 617-632, 1985.

Zarco-Tejada P.J., Berni J.A.J., Suárez L.: Imaging chlorophyll fluorescence with an airborne narrow-band multispectral camera for vegetation stress detection. – Remote Sens. Environ. **113**: 1262-1275, 2009.

Ziegmann M., Abert M., Müller M. *et al*.: Use of fluorescence fingerprints for the estimation of bloom formation and toxin production of *Microcystis aeruginosa*. – Water Res. **44**: 195-204, 2010.